Electronic Supplementary Information

A π-extended benzothiadiazole derivative for high-efficiency TADF-sensitized fluorescent organic light-emitting diode

Guang-Jin Shi,‡[a] Ke-Ke Tan,‡[b] Shu-Yang Liu,[a] Hao Zhang,[a] Hao-Ran Hu,[a] Kun-Peng Wang,[a] Liang-Zhong Xu,[a] Meng Li,*[b] and Zhi-Qiang Hu*[a]

[a]Key Laboratory of Optic-electric Sensing and Analytical Chemistry for Life Science, MOE, College of Chemistry and Molecular Engineering, Qingdao University of Science and Technology, Qingdao, 266042, China.

[b]Beijing National Laboratory for Molecular Sciences, CAS Key Laboratory of Molecular Recognition and Function, Institute of Chemistry, Chinese Academy of Sciences, Beijing 100190, China.

‡These authors contributed equally to this work.

Email: huzhiqiang@qust.edu.cn; limeng@iccas.ac.cn

Contents

1. General information

All reagents were purchased from commercial sources and used without further purification. ^{1}H NMR and ^{13}C NMR spectra were recorded on a Bruker DMX 500 MHz spectrometer. HRMS mass spectra were measured by Waters ACQUITY UPLC H-Class. Theoretical calculations were carried out with software package. Density functional theory (DFT) calculations were performed using the Gaussian 09 package at the B3LYP/6-31G(d) level. Multiwfn and VMD were used for data processing and rendering.[S1]

Absorption spectra were recorded on SHIMADZU UV-2600i spectrophotometer and fluorescence spectra were recorded on SHIMADZU RF-6000 spectrometer at room temperature. The transient PL decay characteristics, delayed PL emission spectra and absolute PLQY were measured on an Edinburgh Instruments FLS 980 spectrometer. Tetrahydrofuran solutions of **BTD-PAH** with a concentration of 10^{-3} M were prepared as stock solutions. Dilute the stock solutions with toluene (PhMe), chloroform ($CHCl_3$), tetrahydrofuran (THF), methyl alcohol (MeOH), dimethyl sulfoxide (DMSO) to the concentration of 10^{-5} μM for measuring absorption, emission spectra and fluorescence lifetime. The absorption wavelength (λ_{abs}), emission wavelength (λ_{em}), molar extinction coefficient (ε), Stokes shifts ($\Delta\lambda$) were calculated by the measurement data. The fluorescent quantum yield in different solvents were calculated by standard compound (Rhodamine 101 as a standard), according to the following equation: $\Phi_f = \Phi_{ST}(Grad_x/Grad_{ST})(\eta^2_x/\eta^2_{ST})$. The subscripts *ST* and *X* denote is standard compound and test compound respectively, Φ_f is the Relative fluorescent quantum yield, *Grad* is the gradient from the plot of integrated fluorescence intensity *vs* absorbance, and η is the refractive index of the solvent.

The OLED devices were fabricated by vacuum deposition onto pre-coated ITO glass substrates at a low pressure (1×10^{-5} mbar) for organic and metal deposition successively, with deposition rate of 0.5~3 Å s^{-1}. Before the fabrication of devices, the ITO glass substrates were cleaned with Decon 90, rinsed in ultrapure water and ethanol, dried in an oven at 120 °C, then by plasma cleaning process. The electroluminescence and current-voltage-luminance characteristics of the devices

were measured with a computer-controlled Spectrascan PR 670 spectrophotometer and Keithley 2400 SourceMeter after device packaging.

2. Synthetic procedures and characterized data

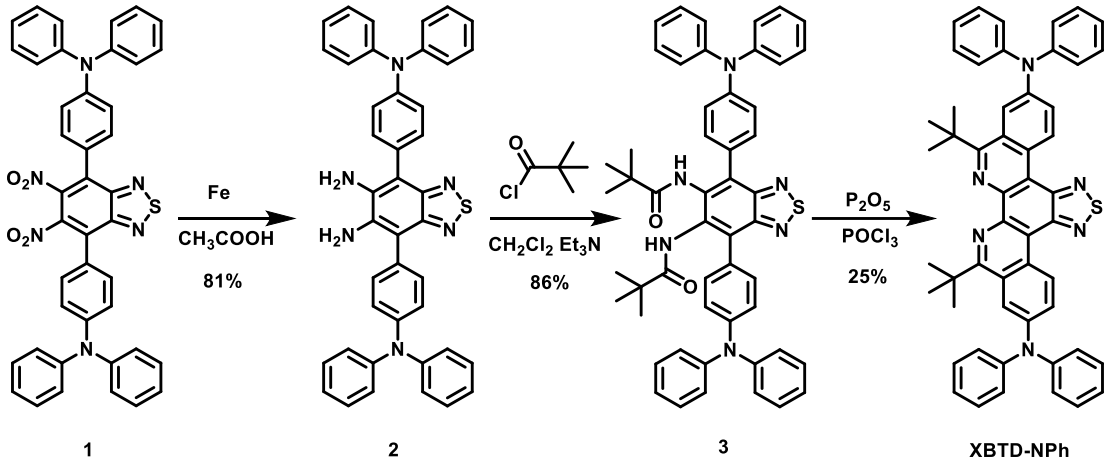

Scheme S1. Synthetic route of **XBTD-NPh**.

The synthetic methods of **1**, **2** and **3** were referred to the reported literature[S2].

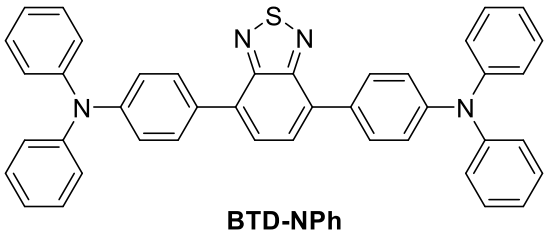

Scheme S2. Molecular structures of **BTD-NPh**.

The synthetic methods of **BTD-NPh** were referred to the reported literature[S3].

***4,7-bis(4-(diphenylamino)phenyl)benzo[c][1,2,5]thiadiazole-5,6-diamine* (2)**

1 (3.56 g, 5 mmol) and reduced iron powder (2.80 g, 50 mmol) were dissolved in 50 mL glacial acetic acid and stirred at 90 °C for 2 h until no **1** was detected by TLC. Added 50 mL water and stirring for another 1 h. After cooling to room temperature, filtered and dried to obtain brown solid **2** (2.64 g, 81%). Proceed directly to the next step without purification.

***N,N'-(4,7-bis(4-(diphenylamino)phenyl)benzo[c][1,2,5]thiadiazole-5,6-diyl)bis(2,2-dimethylpropanamide)* (3)**

2 (1.30 g, 2 mmol) was dissolved in 20 mL of dichloromethane, added with triethylamine (0.81 g, 8 mmol), and stirred at 0 °C for 5 min. Pivaloyl chloride (0.48 g, 4 mmol) was slowly added dropwise and stirred for 8 h at room temperature until no **2** was detected by TLC. Removed solvents by rotary evaporator and purified by silica gel column chromatography (EA:PE = 1:8) and **3** was obtained as yellow solid (1.41 g, 86%). ^{1}H NMR (500 MHz, $CDCl_3$) δ = 7.82 (s, 1H), 7.34 (d, J = 7.9 Hz, 2H), 7.20 (t, J = 7.3 Hz, 4H), 7.11 (dd, J = 23.1, 7.7 Hz, 6H), 6.98 (t, J = 6.8 Hz, 2H), 1.07 (s, 9H). ^{13}C NMR (125 MHz, $CDCl_3$) δ = 177.4, 153.3, 148.1, 147.5, 133.0, 131.0, 129.4, 129.1, 127.9, 124.9, 123.4, 122.9, 39.5, 27.5. HRMS: *m/z* $[M+Na]^+$ calcd for $C_{52}H_{48}N_6NaO_2S^+$, theory: 843.3452, found: 843.3471.

5,8-di-tert-butyl-N^3,N^3,N^{10},N^{10}-tetraphenyldibenzo[c,i][1,2,5]thiadiazolo[3,4-f][1,10] phenanthroline-3,10-diamine **(XBTD-NPh)**

3 (820 mg, 1 mmol) was dissolved in 5 mL of phosphorus oxychloride and phosphorus pentoxide (1.41 g, 10 mmol), and reflux for 4 h under nitrogen protection. Cooled to room temperature and slowly added 40% aqueous sodium hydroxide solution until pH = 14. Filtered and purified by silica gel column chromatography (EA:PE = 1:12) and X**BTD-NPh** was obtained as orange solid (196 mg, 25%). ^{1}H NMR (500 MHz, $CDCl_3$) δ = 10.34 (d, J = 9.3 Hz, 1H), 8.16 (d, J = 1.9 Hz, 1H), 7.77 (dd, J = 9.3, 2.0 Hz, 1H), 7.36 (t, J = 7.7 Hz, 4H), 7.30 – 7.23 (m, 4H), 7.14 (t, J = 7.2 Hz, 2H), 1.64 (s, 9H). ^{13}C NMR (126 MHz, $CDCl_3$) δ = 168.3, 153.0, 147.1, 146.0, 141.3, 129.6, 129.2, 129.1, 126.7, 126.3, 125.4, 124.1, 118.2, 115.4, 40.9, 31.3. HRMS: *m/z* $[M+H]^+$ calcd for $C_{52}H_{45}N_6S^+$, theory: 785.3421, found: 785.3417.

3. Thermal properties

The thermal stability of **XBTD-NPh** was then investigated. Thermogravimetric analyses (TGA) were performed on a TA Instruments Q-50 with a heating rate of 10 °C min^{-1} at N_2 atmosphere. Differential scanning calorimetry (DSC) curves were performed on Netzsch DSC 204F1 at a heating rate of 10 °C min^{-1} at N_2 atmosphere. The result was shown as in Fig. S1.

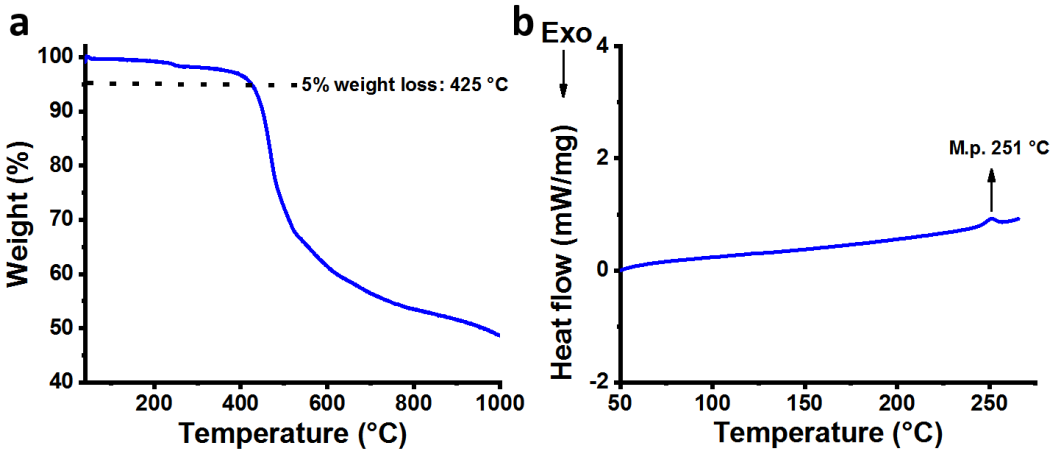

Fig. S1 (a) TGA and (b) DSC curve of X**BTD-NPh**.

4. Theoretical calculations

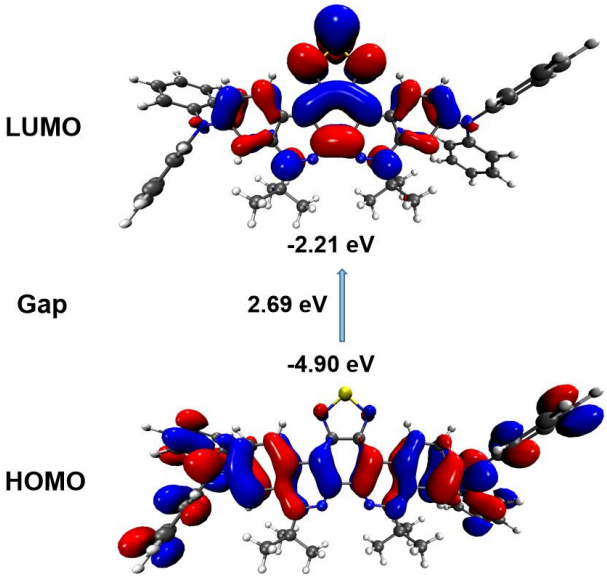

Fig. S2 HOMO/LUMO distributions and energy levels of **XBTD-NPh**.

5. Electrochemical measurements

A conventional three electrode cell was used as electrolytic cell with a glassy carbon working electrode, an Ag/Ag^+ (0.01 M $AgNO_3$) as the reference electrode, and Pt wire as the counter electrode. The oxidation potential was measured in CH_2Cl_2 with 0.1 M of tetra-nbutylammonium hexafluorophosphate (*n*-Bu_4NPF_6) as a supporting electrolyte. Ferrocene used as internal standard for calibrating the reference electrode.

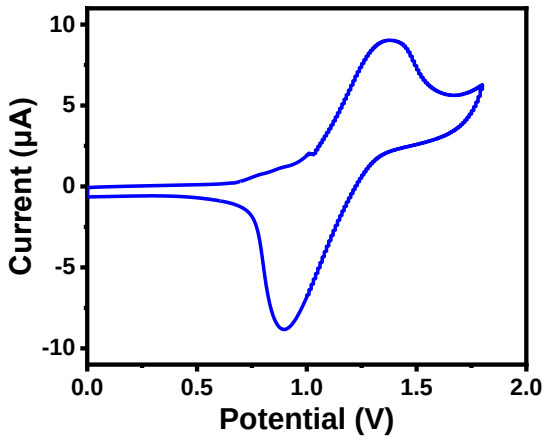

Fig. S3 Cyclic voltammogram of **XBTD-NPh**

Table S1. Electrochemical properties of **XBTD-NPh**

$E_{ox,onset}$[a]	E_{HOMO}[b]	E_{LUMO}[c]	$E_{g,opt}$[d]	λ_{onset}[e]
0.99 eV	–5.64 eV	–3.21 eV	2.43 eV	510 nm

[a]The onset of oxidation curve; [b]$E_{HOMO} = -[E_{ox} - E_{(Fc/Fc+)} + 4.8]$ eV; [c]$E_{LUMO} = E_{HOMO} + E_{g,opt}$; [d]energy gap ($E_{g,opt} = 1240 / \lambda_{onset}$); [e]energy gap ($E_{g,opt} = 1240 / \lambda_{onset}$); [e]the onset of the absorption spectrum.

6. Photophysical properties

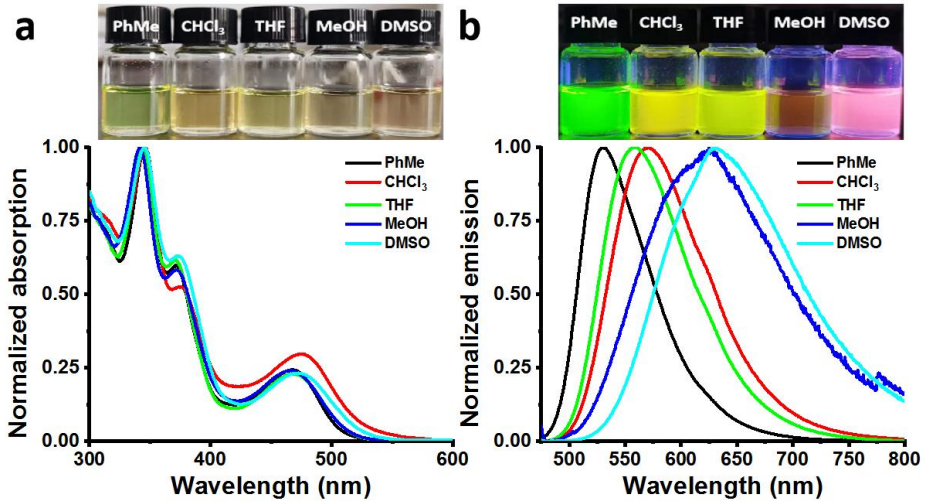

Fig. S4 (a) UV-Vis absorption and (b) emission spectra of **XBTD-NPh** (λ_{ex} = 470 nm) in different solutions ($c = 1 \times 10^{-5}$ M).

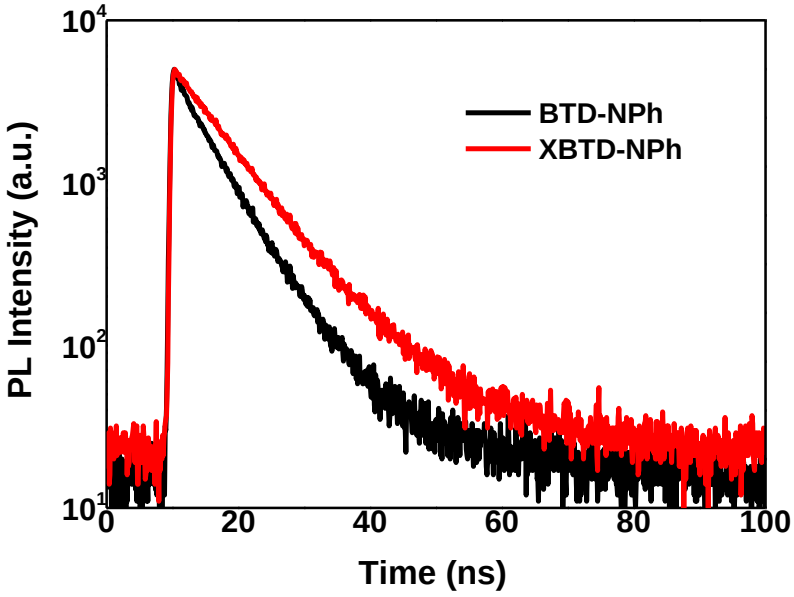

Fig. S5 Transient PL decay of **XBTD-NPh** and **XBTD-NPh** in toluene (c = 1×10^{-5} M) at room temperature.

Table S2. Photophysical properties of **XBTD-NPh** in different solvents

solvents[a]	$\lambda_{abs,max}$ (nm)	λ_{em} (nm)	$\Delta\lambda^b$ (nm)	ε (10^4 M^{-1} cm^{-1})	$\Phi_f{}^c$ (%)	τ_f (ns)
PhMe	468	531	63	0.9	98	9.1
$CHCl_3$	475	571	96	1.1	67	
THF	468	560	92	0.8	87	
MeOH	469	630	161	0.9	3	
DMSO	470	631	161	0.8	21	

[a]Measured at room temperature (c = 1×10^{-5} M); [b]$\Delta\lambda = \lambda_{em} - \lambda_{abs,max}$; [c]Rhodamine 101 as a standard (excited at 450 nm, Φ_f = 0.96 in ethanol)[S4].

7. OLEDs performances

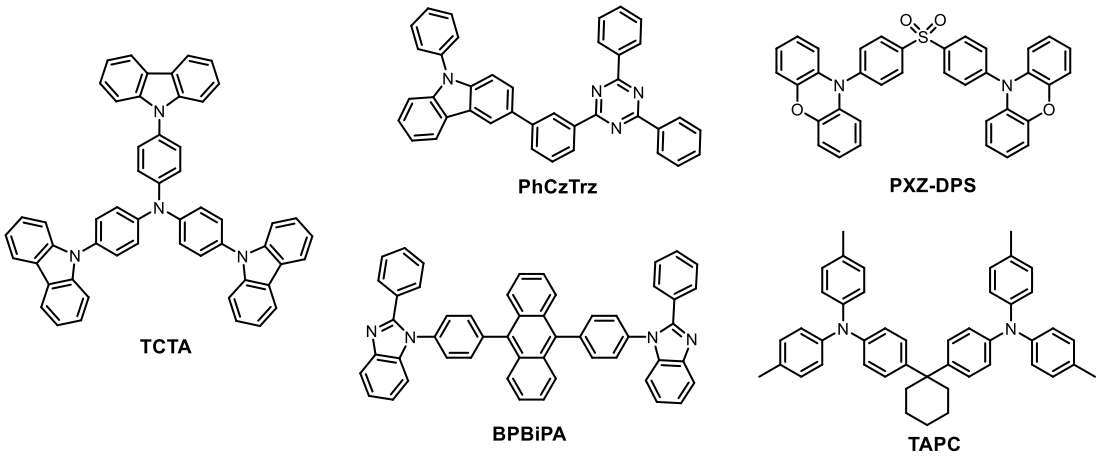

Fig. S6 The molecular structures of the compounds used in the device.

The CP-OLEDs had the structure: Glass/ITO/ TAPC (40 nm)/ TCTA (10 nm)/PhCzTrz : 10 wt% PXZ-DPS : 1.0 wt% **XBTD-NPh** (20 nm)/BPBiPA (40 nm) LiF (0.5 nm)/Al (150 nm). In which, ITO is indium tin oxide, 1,1-bis[4-[*N*,*N*-di(*p*-tolyl)-amino]phenyl]cyclohexane (TAPC) was used as hole-transporting layer, 4,4',4"-Tris(carbazol-9-yl)-triphenylamine (TCTA) was acted as electron-blocking layer, 3-(3-(4,6-diphenyl-1,3,5-triazin-2-yl)phenyl)-9-phenyl-9*H*-carbazole (PhCzTrz) was employed as host material, 10,10'-(sulfonylbis(4,1-phenylene))bis(10*H*-phenoxazine) (PZX-DPS) was served as TADF sensitizer, 1.0 wt% **XBTD-NPh** was co-deposited with PhCzTrz and 10 wt% PXZ-DPS to serve as the emitting layer, 9,10-bis(4-(2-phenyl-1*H*-benzo[*d*]imidazol-1-yl)phenyl)anthracene (BPBiPA) was used as electron-transporting layer, LiF and Al acted as electron-transporting layer, electron-injection layer and the cathode, respectively.

8. ^{1}H NMR, ^{13}C NMR and HRMS of new compounds

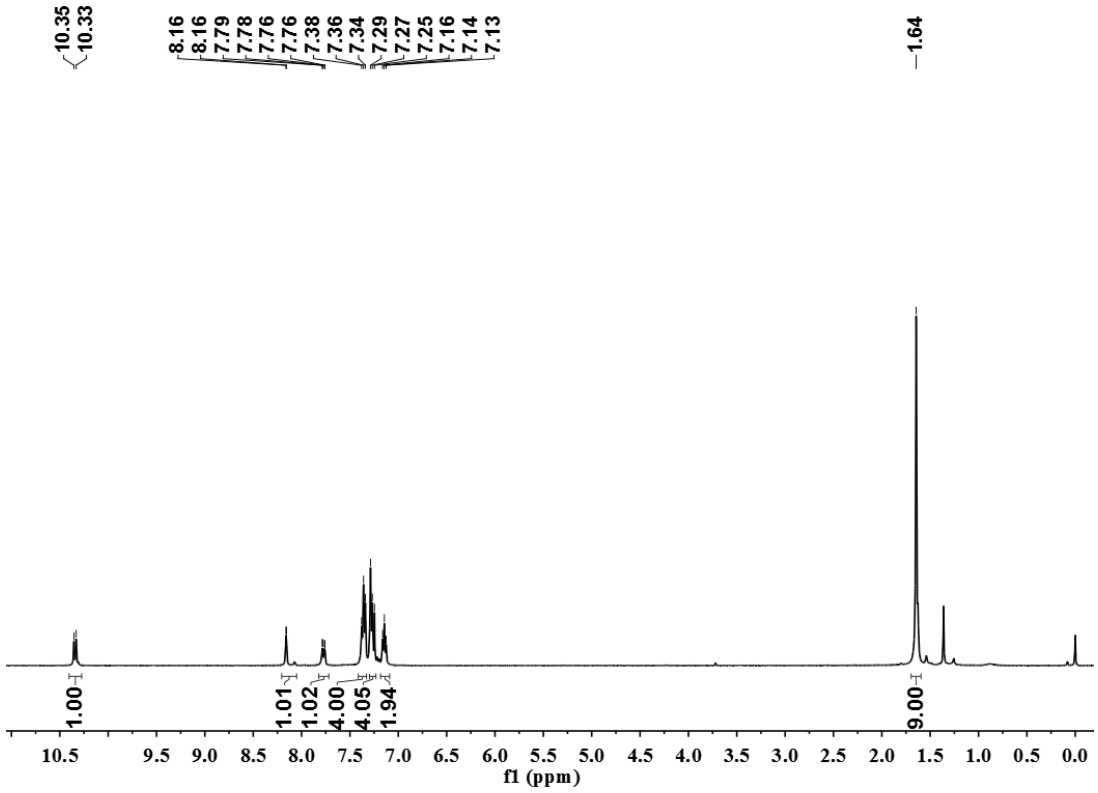

Fig. S7 ^{1}H NMR spectrum (500 MHz, $CDCl_3$) of **XBTD-NPh**.

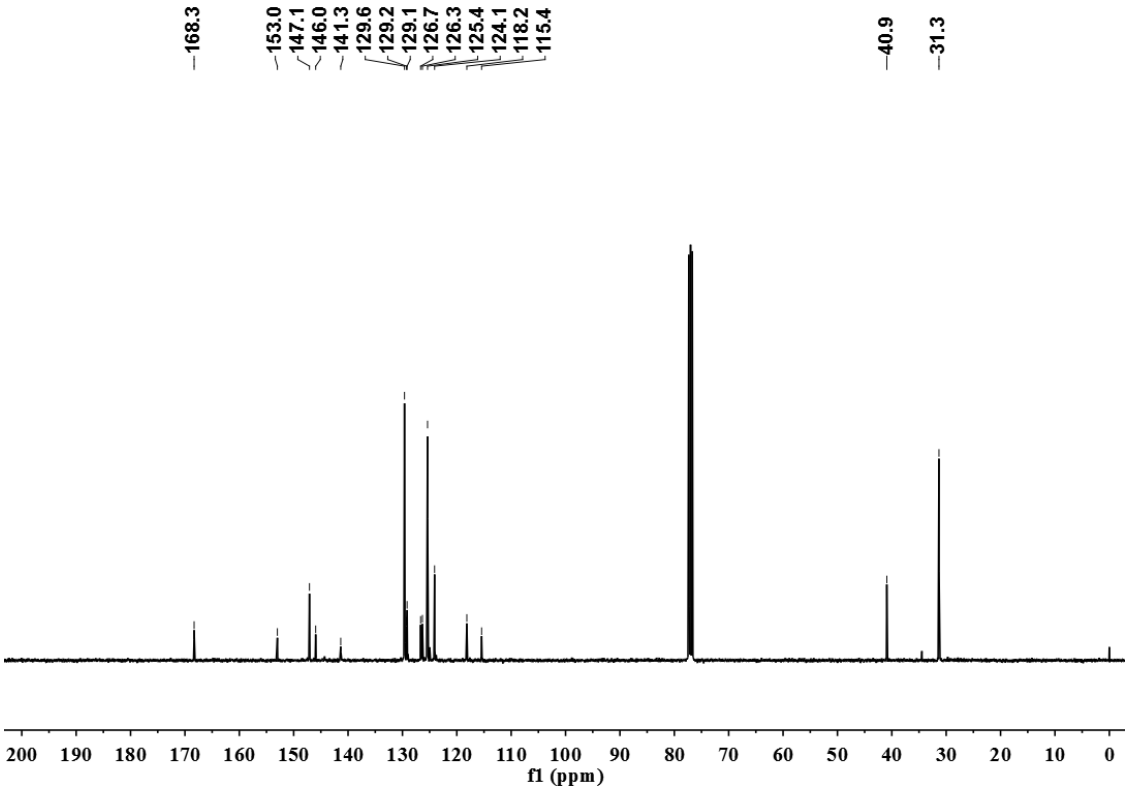

Fig. S8 ^{13}C NMR spectrum (126 MHz, $CDCl_3$) of **XBTD-NPh**.

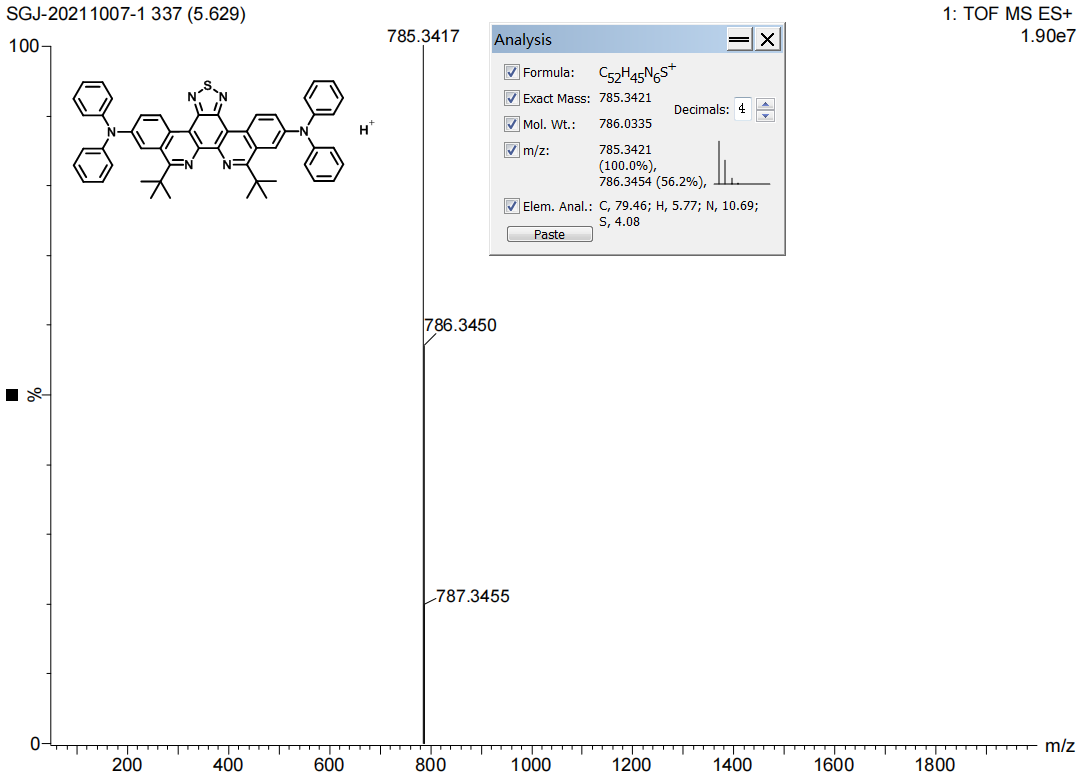

Fig. S9 HRMS of **XBTD-NPh**.

9. References

[S1] (a) T. Lu, and F. Chen, *J. Comput. Chem.* 2012, **33**, 580; (b) W. Humphrey, A. Dalke, and K. Schulten, *J Molec Graphics* 1996, **14**, 33.

[S2] G.-J. Shi, Y.-D. Wang, Z.-X. Yu, Q. Zhang, S. Chen, L.-Z. Xu, K.-P. Wang and Z.-Q. Hu, *Dye. Pigment.*, 2022, **204**, 110471.

[S3] W. Fu, H. Chen, Y. Han, W. Wang, R. Zhang and J Liu, *New J. Chem.*, 2021, **45**, 19082.

[S4] R. F. Kubin and A. N. Fletcher, *J. Lumin.*, 1982, **27**, 455.